



AN ENHANCED SCHT BASED ALAMOUTI SCHEME OVER MULTIPATH CHANNELS

Ambika Annavarapu, Padmavathi Kora and Priyanka Yadlapalli

Department of Electronics and Communication Engineering, GRIET, India

E-Mail: ambika@griet.in

ABSTRACT

This paper introduces an innovative methodology of Orthogonal Space Time Block Coding (OSTBC) based on Multiple Input - Multiple Output (MIMO) using Alamouti - Sequency ordered Complex Hadamard Transform (SCHT) techniques, in order to attain high - speed data communications through wireless media. The outcomes attained through this system compare with other techniques of Alamouti based OSTBC and Conventional OSTBC techniques. In this paper, the Alamouti - Sequency ordered Complex Hadamard Transform (SCHT) based OSTBC - MIMO with 2×2 transmitter-receiver antenna system, for different digital modulation techniques like BPSK (Bipolar Phase Shift Keying) and QPSK (Quadrature Phase Shift Keying) are considered to reduce the Rayleigh fading effect. Using Complex Rademacher matrices (CRM), SCHT is implemented to achieve fast algorithm. A substantial enhancement of bit error rate (BER) for an Alamouti - SCHT - OSTBC based 2×2 transmit - receive antenna system using BPSK and QPSK modulation is perceived from simulation results. From the tabulated results it is obvious that the BER for both QPSK and BPSK are reduced considerably.

Keywords: MIMO, SCHT, ALAMOUTI, OSTBC.

1. INTRODUCTION

Transceiver algorithms for MIMO systems [8] may be generally categorized into two classifications, i.e., those intended to proliferate the transmission rate and those premeditated to increase reliability. The earlier are often communally stated to as spatial multiplexing and the later as transmit diversity. In the diversity - multiplexing trade - off curve, either one of the two extremities is occupied by transmit diversity techniques and spatial multiplexing. Spatial multiplexing provides maximum multiplexing gain at fixed Bit Error Rate (BER) while transmitting diversity techniques provide maximum diversity gain for fixed transmission rate.

Using different diversity schemes improvement in diversity can be achieved in MIMO technology in the Rayleigh fading environment. As the count of transmitting and receive antennas is increased the diversity is upgraded. Only two transmit antennas are only used because as the number of antennas are increased full rate power cannot be achieved. This is further advanced by applying OSTBC technique to MIMO [4]. OSTBC [12] achieves maximum diversity, maximum transmission rate with maximum diversity. OSTBC achieves both space and time diversity to improve MIMO. But at present due to high data rate requirement with lowest fading effect diversity is further needed to be increased. This can be achieved by applying different techniques like Alamouti technique [11] which is introduced by Alamouti in the year of 1998. Alamouti - OSTBC [1] diversity technique is the most fruitful phenomena used to confront the fading of a channel in a wireless environment. But due to the rapid development of digital technology application of fast algorithms to this Alamouti - OSTBC [2] is required. Various fast algorithms like Haar transform (HaT) [10], the Discrete Wavelet Transform (DWT), the Karhunen-Loeve transform (KLT) [13] [14], and the discrete cosine transform (DCT) [9] are used for diversity improvement. The DFT performs the

signal conversion from time to frequency domain for some of the applications. The DCT is widely held for its loftier energy compaction property because a great division of the average energy of the signal is grouped into a comparatively a small number of constituents of the DCT coefficients. It is often used in data and image compression. The DWT is familiar for its analysis for image signal processing in a multiresolution pattern. In the real - time applications, the advanced fast algorithm that is used is Hadamard transform (HT) [5]. The advantage of applying HT to Alamouti - OSTBC is it is a having very low computational complexity of order $O(\log_2 M)$ for M data samples.

The BIFORE (Binary Fourier Representation) or HADAMARD transform [6] contains two levels (± 1). It is used in various applications like signal processing, data compression algorithms, data encryption, quantum computing, etc. But the disadvantage of using this real Hadamard transform is it can be applied only to real values. This limitation can be avoided by using Complex Hadamard transform (CHT) [7]. CHT is a four - valued ($\pm 1, \pm j$) sequence. CHT [15] includes high ordered matrices and Kronecker products. Complex Hadamard Transform with sequency order is called SCHT [3]. Sequency measures how fast the elements of a specific row vector of the Hadamard transform matrix vary over a normalized time base $t \in [0, 1)$.

In this paper, the Alamouti based OSTBC - MIMO with 2×2 transmit - receive antenna system is considered to improve the capability of reducing Rayleigh fading effect. A random signal is considered and modulated with BPSK and QPSK. In addition, SCHT is applied to this technique to improve the bit error rate of an MIMO system as shown in Figure-1. At the receiver end, the AWGN added signals is received by an estimator and these signals are decoded before they are demodulated.



The inverse SCHT [17], [18], [19], [20], [21] is performed at the receiver. The BER performance of BPSK and QPSK modulated signals are compared with the simulated

results Alamouti scheme using HT and Alamouti scheme are compared and plotted in Figure-1.

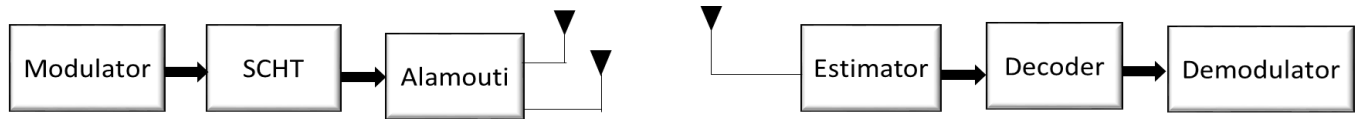


Figure-1. SCHT-Alamouti 2 × 2 OSTBC based MIMO system model.

2. SYSTEM MODELING

The MIMO channel with an input signal s and added AWGN noise of n is in the form:

$$y = Zs + n \quad (1)$$

where s represents the input signal, Z represents the channel matrix, y represents the signal received at the receiver along with the AWGN noise n .

2.1 Space time block codes

An archetype to transmit data over channels affected by Rayleigh fading using multiple antennas is achieved by using Space-time block coding. The data received by STBC is divided into smaller branches and are transmitted using m transmitting antennas. At the receiver antenna, these m signals are added by noise. ML decoding is used for detection at the receiver when the orthogonal design is used for STBC to gain maximum order for diversity with simple decoding algorithms.

2.2 Alamouti scheme

A simple transmit diversity technique called Alamouti is applied on MIMO when there are only two transmitting antennas and any number of receiving antennas as shown in Figure-2. The transmitting antenna number does not exceed two because the full rate power cannot be achieved. If there are M_R number of receiving antennas are there then a maximum of $2M_R$ diversity gain can be achieved at a fixed transmission rate.

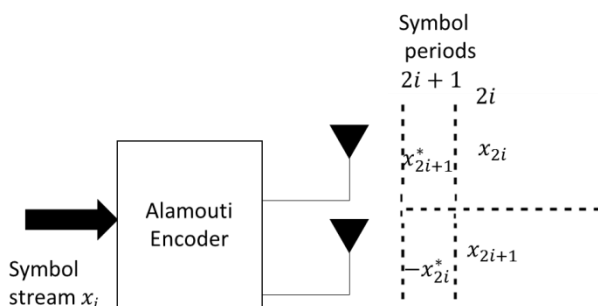


Figure-2. Schematic diagram of Alamouti scheme.

a. Sequence ordered complex Hadamard transform

As the digital devices are occupying a major role in technology a new transformation is required to make the system faster. This can be achieved by using discrete orthogonal transforms. These are used to change the

characteristics of a signal by changing its domain to construe signal without difficulty.

An orthogonal transform called BIFORE or HT is hosted in (2) is established on Walsh functions by taking only two amplitude levels $\{\pm 1\}$ forming a rectangular waveform.

A Hadamard matrix, H_M , is demarcated as a square matrix of dimension $M \times M$ in which 1. All records of a matrix are ± 1 . Any two divergent rows of the matrix are orthogonal, that is,

$$H_M^T H_M = H_M H_M^T = N I_M \quad (2)$$

where H_M^T is the transpose of H_M and I_M is the identity matrix of dimension $M \times M$. In fact, a Hadamard matrix is a symmetric matrix whose row and column vectors are orthogonal to each other. The orthogonality property rests unaffected although the row and column vectors or sign of row and column vectors are exchanged as explained by equation (2).

But the major drawback of HT is it can be applied only to real-valued signals only but in real time applications complex values are also to be considered. So, Hadamard transforms are replaced by a comprehensive form called CHT which comprises the values as $C = \{\pm 1, \pm j\}$ where $j = \sqrt{-1}$. The advantage of CHT is it does not require any additional computational cost because of its complex elements as represented in equations (3) and (4). The orthogonality and simplicity of real HT are not altered because of CHT exclusively trading with complex-valued signals in DSP applications. CHT is constructed on recursive formula comprising the higher order matrix diagonalising and Kronecker product multiples.

Ordered Hadamard matrices are obtained by organizing the rows of matrices in various ways. Sequence order is chosen in all different orderings as it is more equivalent to FT frequency domain representation (3).

In this paper, CHT with sequence ordering called sequence ordered complex Hadamard transforms (SCHTs) are presented. SCHT is a discrete orthogonal transform which is made up of the components $\{\pm 1, \pm j\}$ and the row vectors of the transform matrix are organized in an ascending order of sequence. Sequence order to the number of times that the row vector of a matrix crosses the imaginary axis in the unit circle above a normalized time base $0 \leq k \leq 1$ such that each crossing represent a row of a SCHT matrix. SCHT implementation is modest than



DFT in terms of hardware organization and computational convolution.

SCHT is implemented by using the extended version of conventional Rademacher functions called as complex Rademacher functions (CRD). CRD are used for both odd and even symmetry though they are incomplete orthogonal set of functions with odd symmetry. CRD is defined as follows:

$$CRD(0, k) = g(y) = \begin{cases} 1, & k \in \left[0, \frac{1}{4}\right) \\ j, & k \in \left[\frac{1}{4}, \frac{1}{2}\right) \\ -1, & k \in \left[\frac{1}{2}, \frac{3}{4}\right) \\ -j, & k \in \left[\frac{3}{4}, 1\right) \end{cases} \quad (3)$$

and

$$CRD(0, k+1) = CRD(0, k) \quad (4)$$

where period $K = 1$. Another simpler approach to define CRD over a normalized time base $k \in [0, 1)$ is as follows:

$$CRD(0, k) = e^{-\frac{j\pi csgn(e^{j2\pi kt})}{4\sqrt{2}}} \quad (5)$$

which maps the real-valued t to the element from the set $\{\pm 1, \pm j\}$ where $csgn(y)$ is defined for any nonzero complex number $y = y_1 + jy_2$ as follows:

$$csgn(y) = sgn(y_1) + jsng(y_2) \quad (6)$$

where $sgn(\cdot)$ represents the signum function. But if y is a real number, it can be shown that $csgn(y) = sgn(y)$.

Real Rademacher functions are partially introduced by the complex element j where $j = \sqrt{-1}$ to clench the orthogonality property of the Rademacher functions. For non-negative integer p , the complex Rademacher function series can be defined as follows:

$$CRD(p, k) = CRD(0, 2^p k) \quad (7)$$

where $p = 0, 1, \dots, m-1$. By constricting $CRD(0, k)$ in the horizontal direction by a factor of 2^p results in $CRD(p, k)$. By discretizing the CRD function series the CRD matrices are obtained i.e., sampling the CRD function series at $M = 2^m$ equally spaced locations within the normalized time k . Let R_m be the CRD matrix of dimension $m \times 2m$. Then, the p^{th} row of R_m is defined as

$$R_m(p, l) = CRD\left(p, \frac{l}{2^m} + \frac{1}{2^{m+2}}\right) = CRD\left(p, \frac{4l+1}{2^{m+2}}\right) \quad (8)$$

where $p = 0, 1, \dots, m-1$ and $l = 0, 1, \dots, 2m-1$.

Let us, as an example, consider $M = 8$. Then, the 3×8 complex Rademacher matrix is fashioned in (9) by placing (3) and (4) in (8) and attained values are tabulated in Table-1.

Table-1. Complex Rademacher matrix values for $M = 8$.

| $R_m(p, l)$ \ l | 0 | 1 | 2 | 3 | 4 | 5 | 6 | 7 |
|-------------------|----------|-----------|-----------|-----------|-----------|-----------|------------|------------|
| $R_m(0, l)$ | 1 /32 | 5 /32 | 9 /32 | 13 /32 | 17 /32 | 21 /32 | 25 /32 | 29 /32 |
| $R_m(1, l)$ | 2 /32 | 10 /32 | 18 /32 | 26 /32 | 34 /32 | 42 /32 | 50 /32 | 58 /32 |
| $R_m(2, l)$ | 4 /32 | 20 /32 | 36 /32 | 52 /32 | 68 /32 | 84 /32 | 100 /32 | 116 /32 |

$$R_3 = \begin{bmatrix} 1 & 1 & j & j & -1 & -1 & -j & -j \\ 1 & j & -1 & -j & 1 & j & -1 & -j \\ 1 & -1 & 1 & -1 & 1 & -1 & 1 & -1 \end{bmatrix} \quad (9)$$

Using complex Rademacher matrices [7], the SCHT matrices are engendered based on the products of the row vectors of complex Rademacher matrices. Let H_M be the SCHT matrix of size $M \times M$ where $M = 2^m$. Then, it is defined as

$$H_M(g, l) = \prod_{p=0}^{m-1} R_m(p, l)^{b_p} \quad (10)$$

where $R_m(p, l)$ is the (p^{th}, l^{th}) element of the complex Rademacher matrix,

$$g = b_{m-1}2^{m-1} + \dots + b_12^1 + b_02^0 \quad (11)$$

and $b_p = 0$ or 1 . Let $R_m(p)$, for $p = 0, 1, \dots, m-1$, be the p^{th} row vector of the complex Rademacher matrix. For example, let us consider H_8 (12) which can be achieved by using (10) and the values are tabulated in Table-2. Equation (13) is obtained by substituting equation (3) in (12).

**Table-2.** SCHT matrix $H_8(g, l)$ for $M = 8$.

| g | $H_8(g, l)$ |
|-----|---|
| 000 | 1 |
| 001 | $R_3(0, l)$ |
| 010 | $R_3(1, l)$ |
| 011 | $R_3(1, l) \odot R_3(0, l)$ |
| 100 | $R_3(2, l)$ |
| 101 | $R_3(2, l) \odot R_3(0, l)$ |
| 110 | $R_3(2, l) \odot R_3(1, l)$ |
| 111 | $R_3(2, l) \odot R_3(1, l) \odot R_3(0, l)$ |

$$H_8(g, l) = \begin{bmatrix} 1 \\ R_3(0, l) \\ R_3(1, l) \\ R_3(1, l) \odot R_3(0, l) \\ R_3(2, l) \\ R_3(2, l) \odot R_3(0, l) \\ R_3(2, l) \odot R_3(1, l) \\ R_3(2, l) \odot R_3(1, l) \odot R_3(0, l) \end{bmatrix} \quad (12)$$

$$H_8(g, l) = \begin{bmatrix} 1 & 1 & 1 & 1 & 1 & 1 & 1 & 1 \\ 1 & 1 & j & j & -1 & -1 & -j & -j \\ 1 & j & -1 & -j & 1 & j & -1 & -j \\ 1 & j & -j & 1 & -1 & -j & j & -1 \\ 1 & -1 & 1 & -1 & 1 & -1 & 1 & -1 \\ 1 & -1 & j & -j & -1 & 1 & -j & j \\ 1 & -j & -1 & j & 1 & -j & -1 & j \\ 1 & -j & -j & -1 & -1 & j & j & 1 \end{bmatrix} \quad (13)$$

The positions of binary ones of decimal value g bring into being by the row index values 2, 1 and 0. The input to SCHT is the complex assemblage obtained from the output of PSK which is represented as $\vec{d} = [d_1 d_2 \dots d_m]^T$. SCHT of \vec{d} is given as

$$\vec{x} = H_M \vec{d} \quad (14)$$

where H_M represents the SCHT matrix of size $M \times M$ where $M = 2^m$.

When BPSK modulation is used the signal assemblage contains 0 or 1. These are given to the symbol u but when QPSK modulation is used the signal assemblage contains the combinations 00,01,11,10. The SCHT matrix changes the values as shown in Table-3.

Table-3. SCHT matrix values for QPSK modulation.

| d_1 | d_2 | $(1/2)(d_1 + d_2)$ | $(1/2)(d_1 - d_2)$ |
|-------|-------|--------------------|--------------------|
| 00 | 00 | $-1 - j$ | 0 |
| 00 | 01 | -1 | $-j$ |
| 00 | 11 | $-j$ | -1 |
| 00 | 10 | -1 | $-j$ |
| 01 | 00 | -1 | 0 |
| 01 | 01 | 0 | j |
| 01 | 11 | 0 | $-1 + j$ |
| 01 | 10 | 1 | -1 |
| 11 | 00 | 0 | $1 + j$ |
| 11 | 01 | 1 | j |
| 11 | 11 | $-j$ | 0 |
| 11 | 10 | 1 | $-j$ |
| 10 | 00 | $-j$ | 1 |
| 10 | 01 | 0 | $1 - j$ |
| 10 | 11 | 1 | $-j$ |
| 10 | 10 | $1 - j$ | 0 |

These values are applied to 2×2 Alamouti scheme. This scheme generates two symbols x_1 and x_2 for transmission for first period and symbols $-x_2^*$ and x_1^* for the second period to transmit two symbols all together.

$$x = \begin{bmatrix} x_1 & x_2 \\ x_2^* & -x_1^* \end{bmatrix}, Z = \begin{bmatrix} z_1 & z_3 \\ z_2 & z_4 \end{bmatrix} \quad (15)$$

where $x_1 = d_1 + d_2$ and $x_2 = d_1 - d_2$
The output signal at an antenna is given as

$$\begin{aligned} \begin{bmatrix} y_1 \\ y_2 \end{bmatrix} &= \begin{bmatrix} x_1 & x_2 \\ x_2^* & -x_1^* \end{bmatrix} \begin{bmatrix} z_1 & z_3 \\ z_2 & z_4 \end{bmatrix} + \begin{bmatrix} n_1 & n_3 \\ n_2 & n_4 \end{bmatrix} \\ &= \begin{bmatrix} (d_1 + d_2) & (d_1 - d_2) \\ (d_1 - d_2)^* & -(d_1 + d_2)^* \end{bmatrix} \begin{bmatrix} z_1 & z_3 \\ z_2 & z_4 \end{bmatrix} \begin{bmatrix} n_1 & n_3 \\ n_2 & n_4 \end{bmatrix} \end{aligned} \quad (16)$$

These will be recurrent for the next time slots also which are given as follows:

$$\begin{aligned} \begin{bmatrix} y_3 \\ y_4 \end{bmatrix} &= \begin{bmatrix} x_3 & x_4 \\ x_4^* & -x_3^* \end{bmatrix} \begin{bmatrix} z_5 & z_6 \\ z_7 & z_8 \end{bmatrix} + \begin{bmatrix} n_1 & n_3 \\ n_2 & n_4 \end{bmatrix} \\ &= \begin{bmatrix} (d_3 + d_4) & (d_3 - d_4) \\ (d_3 - d_4)^* & -(d_3 + d_4)^* \end{bmatrix} \begin{bmatrix} z_5 & z_6 \\ z_7 & z_8 \end{bmatrix} + \begin{bmatrix} n_1 & n_3 \\ n_2 & n_4 \end{bmatrix} \end{aligned} \quad (17)$$

By using the above signals, the output at each antenna can

| $BER \backslash E_b/N_0$ | Alamouti [11] | Alamouti - HT [1] | Alamouti - SCHT |
|--------------------------|-----------------------|----------------------|-----------------------|
| 5 dB | 6.0×10^{-2} | 1.0×10^{-2} | 0.25×10^{-2} |
| 10 dB | 1.4×10^{-2} | 4.5×10^{-3} | 1.75×10^{-3} |
| 15 dB | 6.8×10^{-3} | 7.0×10^{-4} | 0.8×10^{-4} |
| 20 dB | 1.15×10^{-3} | 7.6×10^{-5} | 0.9×10^{-5} |



be obtained as

$$\begin{bmatrix} y_1^1 \\ y_2^1 \\ y_1^{2*} \\ y_2^{2*} \end{bmatrix} = \begin{bmatrix} z_{11} & z_{12} \\ z_{21} & z_{22} \\ z_{12}^* & -z_{11}^* \\ z_{22}^* & -z_{21}^* \end{bmatrix} \begin{bmatrix} d_1 + d_2 \\ d_1 - d_2 \end{bmatrix} + \begin{bmatrix} n_1^1 \\ n_2^1 \\ n_1^{2*} \\ n_2^{2*} \end{bmatrix} \quad (18)$$

The original signals are reconstructed from the received signals by using the inverse SCJT as shown below

$$\tilde{x} = H_M^{-1} \tilde{y} \quad (19)$$

By doing the inverse SCJT, the original signal is regenerated at the receiver. Now BER is to be calculated.

3. ERROR PERFORMANCE SIMULATION RESULTS

In this section bit error rate of SCJT - Alamouti based MIMO is calculated at respective SNR values by using following equation

$$BER = \frac{1}{2} \operatorname{erfc} \left(\sqrt{\frac{E_b}{N_0}} \right) \quad (20)$$

By considering the following Figure-3 and TABLE IV, it is observed that the Alamouti - SCJT achieved a drastic diminution of BER compared to the Alamouti and Alamouti - HT using BPSK modulation. These bit error rates can be further reduced when the modulation technique is changed to QPSK as shown in the TABLE V and Figure-4.

For BPSK modulation Alamouti - SCJT achieves a BER of 1.0×10^{-4} at 15 dB, Alamouti - HT has 5.0×10^{-3} and 6.0×10^{-3} for Alamouti scheme. This is can be further reduced by Alamouti - SCJT to 0.8×10^{-4} for QPSK modulation.

Table-4. Simulation results for BPSK modulation.

| $\frac{BER}{E_b/N_0}$ | Alamouti [11] | Alamouti - HT [1] | Alamouti - SCJT |
|-----------------------|----------------------|----------------------|----------------------|
| 5 dB | 6.4×10^{-2} | 6.0×10^{-2} | 0.3×10^{-2} |
| 10 dB | 1.4×10^{-2} | 1.2×10^{-2} | 1.8×10^{-3} |
| 15 dB | 6.0×10^{-3} | 5.0×10^{-3} | 1.0×10^{-4} |
| 20 dB | 1.2×10^{-3} | 1.1×10^{-3} | 1.0×10^{-5} |

Table-5. Simulation results for QPSK modulation.

| $\frac{BER}{E_b/N_0}$ | Alamouti [11] | Alamouti - HT [1] | Alamouti - SCJT |
|-----------------------|-----------------------|----------------------|-----------------------|
| 5 dB | 6.0×10^{-2} | 1.0×10^{-2} | 0.25×10^{-2} |
| 10 dB | 1.4×10^{-2} | 4.5×10^{-3} | 1.75×10^{-3} |
| 15 dB | 6.8×10^{-3} | 7.0×10^{-4} | 0.8×10^{-4} |
| 20 dB | 1.15×10^{-3} | 7.6×10^{-5} | 0.9×10^{-5} |

BER for BPSK modulation with 2x2 MIMO with SCJT-Alamouti scheme(Rayleigh channel)

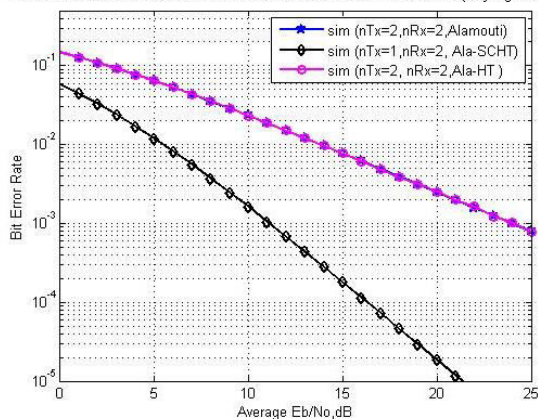


Figure-3. Comparison of BER of SCJT-Alamouti, Alamouti-HT and Alamouti schemes for BPSK modulation.

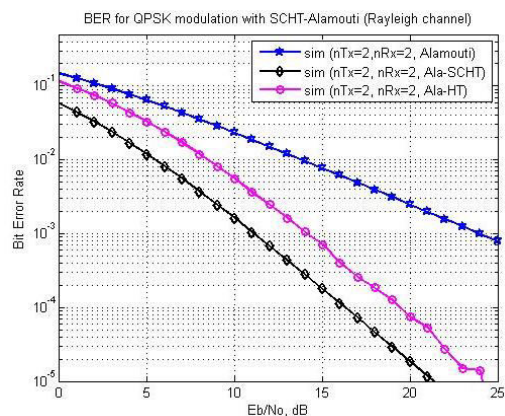


Figure-4. Comparison of BER of SCJT-Alamouti, Alamouti-HT and Alamouti schemes for QPSK modulation.



4. CONCLUSIONS

In this paper a new transmit diversity scheme has been offered. It is shown that, using 2×2 transmit - receive antenna system a strong bit error rate performance is assured. By means of the mathematical simulations it is acquired that the SCHO based Alamouti - OSTBC system applied to MIMO using BPSK and QPSK circumstances achieves high performance by reducing the BER compared to the Alamouti based MIMO and Alamouti - HT [1] based 2×2 MIMO systems.

REFERENCES

- [1] Thomhert Suprpto Siadari, Soo Young Shin. 2014. Joint Hadamard transform and Alamouti scheme for wireless communication system. International Journal of Electronics and Communications (AEU). 68: 889-891.
- [2] K.O.O. Anoh, O. Ochonogor, R.A.A. Abd-Ahameed, S.M.R. Jones. 2014. Improved Alamouti STBC Multi-Antenna System Using Hadamard Matrices. Int. J. Communications, Network and System Sciences. 7: 83-89.
- [3] A. Aung, B.P. Ng and S. Rahardja. 2008. Sequency-Ordered Complex Hadamard Transform: Properties, Computational Complexity and Applications. IEEE Transactions on Signal Processing. 56(8): 3562-3571.
- [4] Ambika. Annavarapu, E. Adi Narayana. 2012. Matlab Simulation for Diversity and Performance Enhancement of OSTBC-CDMA System Using Channel Coding Techniques over Multipath. International Journal of Engineering and Science Research. 2(11): 1842-1850.
- [5] N. Ahmed, K. R. Rao, Abdussattar. 1971. BIFORE or Hadamard. IEEE Trans. Audio Electroacoust. AU-19(3): 225-234.
- [6] Hershey. J, R. Yarlagadda. 1997. Hadamard Matrix Analysis and Synthesis with Applications to Communications and Signal/Image Processing. Norwell, MA: Kluwer.
- [7] Rahardja. S, B.J. Falkowski. 2004. Complex Hadamard transforms: Properties, relations and architecture. IEICE Trans. Fundam. Electron. Commun. Comput. Sci. E87A (8): 2077-2083.
- [8] Daniel W. Bliss, Keith W. Forsythe and Amanda M.Chan. 2005. MIMO Wireless Communication. Lincoln Laboratory Journal. 15(1): 97-126.
- [9] Ahmed. N, Natarajan. T, Rao. 1974. K.R Discrete Cosine Transform. Computers, IEEE Transactions. C-23(1): 90-93.
- [10] Radomir S. Stankovica, Bogdan j. Falkowskib. 2003. The Haar Wavelet Transform: its status and achievements. Computers and Electrical Engineering. 29(1): 25-44.
- [11] Alamouti. S.M. 1998. A simple transmit diversity technique for wireless communications. IEEE Journal on Select Areas in Communications. 16: 1451-1458.
- [12] Tarokh V, Jafarkhani H, Calderbank AR 1999. Spacetime block codes from orthogonal designs. IEEE Transactions on Information Theory. 45: 1456-1467.
- [13] L. Torres-Urgell, R. Lynn Kirlin. 1990. Adaptive image compression using Karhunen-Loeve transform. Signal Processing. 21(4): 303-313.
- [14] M. Effros, F. Hanying, K. Zeger. 2004. Suboptimality of the Karhunen-Loeve transform for transform coding. IEEE Trans, Inf. Theory. 50(8): 1605-1619.
- [15] Ahmed. N, K.R. Rao. 1971. Complex BEFORE transforms. Int. J. Syst, Sci. 2(2): 149-162.
- [16] Hasan Md Mahmudul. 2012. Performance Comparison of Wavelet and FFT Based Multiuser MIMO OFDM over Wireless Rayleigh Fading Channel. International Journal of Energy, Information and Communications. 3.4.
- [17] Padmavathi Kora, K. Sri Rama Krishna. 2016. ECG Based Heart Arrhythmia Detection Using Wavelet Coherence and Bat Algorithm" Sensing and Imaging, Springer. 17(1), June.
- [18] Ambika Annavarapu, Padmavathi Kora, "ECG-based atrial fibrillation detection using different orderings of Conjugate Symmetric-Complex Hadamard Transform," International Journal of Cardiovascular Academy, Elsevier, Aug 2016. 10.1016/j.ijcac.2016.08.001
- [19] Padmavathi Kora, Ambika Annavarapu, Priyanka Yadlapalli, Nagaja Ktragadda. 2016. Classification of Sleep Apnea using ECG-Signal Sequency Ordered Hadamard Transform Features" International Journal of Computer Applications. 156(14): 7-11, December.
- [20] Padmavathi Kora. 2016. Sudden Cardiac Death (SCD) Prediction based on Fast Sequency Ordered Complex Hadamard Transform, International Journal of Computer Applications. 156(14): 1-6, December.
- [21] Padmavathi Kora, Ambika Annavarapu, K. Sri Ramakrishna, Viswanadha Raju Somalaraja, Priyanka Yadlapalli. 2017. Atrial Fibrillation detection using Fast Sequency Ordered Complex Hadamard Transform and Hybrid Firefly Algorithm", Engineering Science and Technology, an International Journal. vol. 20, February.